Design and characterization of an OPV-ETFE multi-layer semi-transparent glazing

Alex Moreno, Alberto Riverola, Daniel Chemisana, Rodolphe Vaillon, Alejandro Solans

▶ **To cite this version:**

Alex Moreno, Alberto Riverola, Daniel Chemisana, Rodolphe Vaillon, Alejandro Solans. Design and characterization of an OPV-ETFE multi-layer semi-transparent glazing. Energy Reports, 2022, 8, pp.8312-8320. 10.1016/j.egyr.2022.06.036 . hal-03710072

HAL Id: hal-03710072
https://hal.science/hal-03710072

Submitted on 30 Jun 2022

HAL is a multi-disciplinary open access archive for the deposit and dissemination of scientific research documents, whether they are published or not. The documents may come from teaching and research institutions in France or abroad, or from public or private research centers.

L'archive ouverte pluridisciplinaire **HAL**, est destinée au dépôt et à la diffusion de documents scientifiques de niveau recherche, publiés ou non, émanant des établissements d'enseignement et de recherche français ou étrangers, des laboratoires publics ou privés.

Published in Energy Reports
https://doi.org/10.1016/j.egyr.2022.06.036

Design and characterization of an OPV-ETFE multi-layer semi-transparent glazing

A. Moreno[1], A. Riverola[1], D. Chemisana[1,*], R. Vaillon[2], A. Solans[1]

[1] Applied Physics Section of the Environmental Science Department
University of Lleida, 25001 Lleida, Spain.
[2] IES, Univ Montpellier, CNRS, Montpellier, France.

*correspondence: daniel.chemisana@macs.udl.cat

Abstract

Architectural glazing has several advantages in terms of aesthetics and user well-being perspectives. However, they can have large impacts on heating and cooling demands and artificial lighting requirements. Ethylene tetrafluoroethylene (ETFE) cushion systems present adequate insulating and transparency characteristics, and, combined with organic photovoltaic (OPV) modules, become a glazing element leading towards energy efficient buildings. The present manuscript reports on a detailed optical, thermal and electrical analysis of a 3-layer ETFE / OPV cushion that helps the design of these glazing-type systems by providing a better understanding of their performance. Spectrophotometric optical measurements up to 50 μm allow proper estimations of an individual layer radiative behavior. As a matter of fact, these measurements feed the radiative and thermal models that aim at determining the behavior of the organic photovoltaic module as a function of its position in the cushion. Based on the organic photovoltaic module spectral response, electrical power production is estimated. Results reveal that the best configuration is the one placing the organic photovoltaic module in the outer layer, since it represents the case where the OPV module performs better due to the higher incident irradiance and the low dependency on temperature of the generated power.

Keywords: Solar energy, building integrated photovoltaics, organic photovoltaics, polymeric membranes, semi-transparent glazing, spectral selection.

1 Introduction

Buildings weight 40% of the overall energy consumption in the European Union (EU). This is partly because 75% of the EU's buildings are energy inefficient [1]. Although a better insulation could lead to building energy savings, architectural concepts tend to increase the glazing fraction of the building envelope. Glazing elements need to be carefully designed since they have a large impact on building energy demands, including space heating and cooling, and artificial lighting requirements. From a positive perspective, glazing has an influence on sustaining human health and well-being [2]. Even though technological progress in developing more efficient glazing systems is undergoing, their thermal properties remain a weak point, provoking higher cooling demands in summer and higher heating demands in winter [3].

In order to move forward, a Directive of the European Parliament (2018/844) specifically defines the objectives to be fulfilled in buildings by 2030: energy efficiency should be improved by 32.5%, greenhouse gas emissions should be reduced by 40%, and 32% of energy production should come from renewable energy [4]. These EU Directive goals should be met by integrating renewable energies and by incorporating energy efficient materials in the building envelope, especially those involved in architectural glazing.

Among renewable energies, solar energy stands as the one with the greatest potential since the solar resource is the most extended. Specifically, photovoltaic (PV) modules represent one of the most efficient and practical ways to convert solar energy into electricity [5]. In the frame of building integrated photovoltaics, transparent or semi-transparent photovoltaics technologies extend building integration possibilities to glazing elements [6]. Semitransparent Organic photovoltaic (ST-OPV) modules present interesting features such as lightness, free-form, flexibility, cost-effectiveness, that make them a great candidate for building integration applications. ST-OPVs achieve power conversions efficiencies ranging from 12% to 14% with an average transmittance of 9–25% in the visible range [7]. It should also be highlighted that OPVs have a very low environmental impact and short energy payback times [8].

Regarding architectural glazing, traditional glass-based systems are being gradually replaced by polymeric foils and membranes, especially in building applications such as transparent roofs and atria [9], sport stadiums double skins, commercial centers, etc. [9]–[13]. One of the most used polymers is ethylene tetrafluoroethylene (ETFE) due to its adequate properties (mechanical resistance, stability, transparency, self-cleaning, reduced environmental impact,

etc.) for being an architectural material. An in-depth analysis of the ETFE characteristics is reported in [14].

Based on the aforementioned characteristics of both OPV modules and ETFE foils or membranes, a promising strategy is to integrate both elements within a PV glazing system. In fact, during the last decade several authors conducted research on this type of combination. Researchers from Politecnico Di Milano presented the concept of integrating OPVs in ETFE cushion elements in 2012 [15]. The same group analyzed the electrical-mechanical performance of a single OPV-ETFE layer [16]. Hu *et al*. [17] investigated the electrical and mechanical properties of OPVs directly printed on ETFE foils. Experimental observations showed that the electrical properties are relatively independent of mechanical loads but that thermal-mechanical properties are closely related to each other. Menéndez *et al*. [18] developed a standardized ETFE module acting as a flexible LED display powered by OPVs. Results proved that OPVs can cover partly the LED display electrical consumption. The most recent study found in the literature analyzing an OPV-ETFE glazing deals with the dynamic energetic simulation and luminous performance of a building façade system [19]. It consists of a planar 2-layer window, where the OPVs are placed in the internal ETFE layer. Different window-to-wall ratios and configurations were assessed for two different locations, Barcelona and Paris, and the influence on the heating and cooling demands and on the illumination levels, with respect to a reference glazing case, was analyzed. The simulated results showed some improvements, to a greater or lesser extent depending on the configuration, in all the analyzed figures of merit. As indicated above, several studies studied similar ETFE-OPV configurations, either for planar or curved (cushion) geometries, indicating the potential uses of such a combination for building integration.

In light of the investigations mentioned above, there is no study analyzing the spectral performance of ETFE-OPV architectural membranes from the ultraviolet to the mid- infrared. The largest wavelength considered is usually 2500 nm. However, operating temperatures of building glazing elements are usually in the range 10-50 ºC. This means that thermal exchange occurs at wavelengths much longer than 2500 nm. In order to fill this important gap, the present research deals with the radiative and thermal modelling of ETFE-OPV membranes covering the spectral range 0.35-50 μm for the radiative properties. The electrical output of the OPVs is included in the model in order to perform a complete analysis of the optical, thermal and electrical performances. The manuscript begins by describing the methods used in the

investigation (Section 2). The results obtained by means of applying such methods are included in Section 3. Finally, the main conclusions the study are stated.

2 Methods

This section aims at describing the three main analyses carried out in the present research: experimental optical characterization of the ETFE-OPV elements, modelling of emittance and thermal behavior of three-layer cushions.

2.1 Optical measurements

The spectral transmittance ($T(\lambda)$) and reflectance ($R(\lambda)$) of ETFE foils (150 and 200 µm thick) and commercially available OPVs fabricated by InfinityPV [20] were determined from 0.35 to 50 µm with a FTIR (Fourier-transform infrared) spectrometer Bruker Optics—IFS 66 v/S equipped with an integrating sphere. This spectral range covers both the solar range and almost the full range of thermal emission (> 99% for 25 °C) in the mid-infrared range for common operational temperatures. The measurements were carried out at room temperature and considered to be valid over the operating range [21]. Using Kirchhoff's law, the spectral absorptance (A(λ)) or emittance (E(λ)) can be derived from the experimental measurements as follows:

$$E(\lambda) = A(\lambda) = 1 - R(\lambda) - T(\lambda) \quad (1)$$

The measured optical characteristics of the ETFE foils and the OPV module are depicted in Figures 1 and 2.

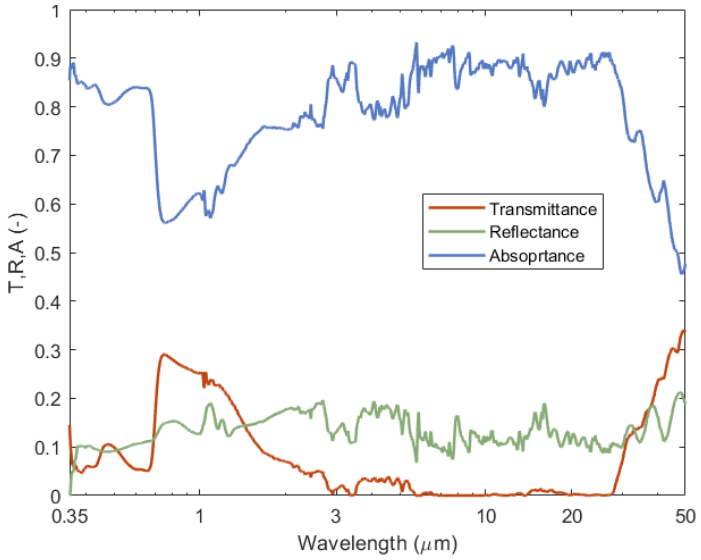

Figure 1. OPVs' spectral (from 0.35 to 50 µm) optical properties measured under normal incidence.

Figure 1 shows the spectral reflectance, transmittance and absorptance of the OPVs under normal incidence. As expected from an organic PV module, OPVs are highly absorptive from the ultraviolet up to 0.65 µm (the range where photovoltaic conversion takes place). At around 0.65 µm, there is a sharp decrease in absorptance from 0.84 to 0.57. From 0.65 µm to almost 30 µm, the absorptance grows from 0.57 to 0.9 just before decreasing again. The reflectance fluctuates a little over the whole spectral interval around an average value of 13%.

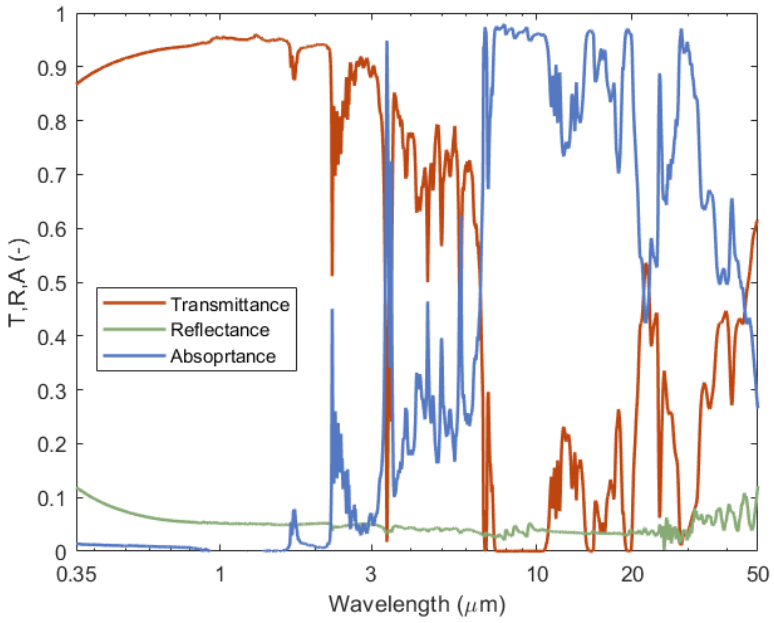

Figure 2. ETFE optical properties (150 µm-thick) measured under normal incidence

The spectral reflectance, transmittance and absorptance of the 150 µm-thick ETFE foil are shown in Figure 2. ETFE barely absorbs photons for wavelengths below 2 µm. From 2 µm up to 6.5 µm, absorptance grows steadily from almost 0 to 0.4. Then, it increases up to 30 µm except with a dip at 23 µm. Finally, absorptance decreases from 0.9 to 0.5 between 30 and 50 µm.

Reflectance is almost constant at 0.06 from the ultraviolet to the edge of the mid-infrared range and, therefore, transmittance follows a trend which is opposite to that of absorptance. Nonetheless, ETFE is highly transmissive from the ultraviolet up to 6.5 µm allowing solar radiation to pass through almost unaltered.

In addition, since two ETFE foils with different thicknesses were measured, the complex refractive index ($\acute{n} = n + \hat{\imath}k$) of ETFE was calculated so that it can be used for radiation transfer calculations, using the ray-tracing algorithm described in [22].

ETFE layers and OPVs are very well suited for use as semi-transparent solar envelopes. The ETFE high transmittance over the solar range combined with its high emittance over the atmospheric main transparency window (8 - 13 µm) are key properties for glazing elements. On the other hand, both ETFE and OPV are strong absorbers in the mid-infrared range. Figure 3 shows the ETFE and OPVs' normal emittance values together with the atmospheric transmittance and the AM1.5G solar spectrum [23].

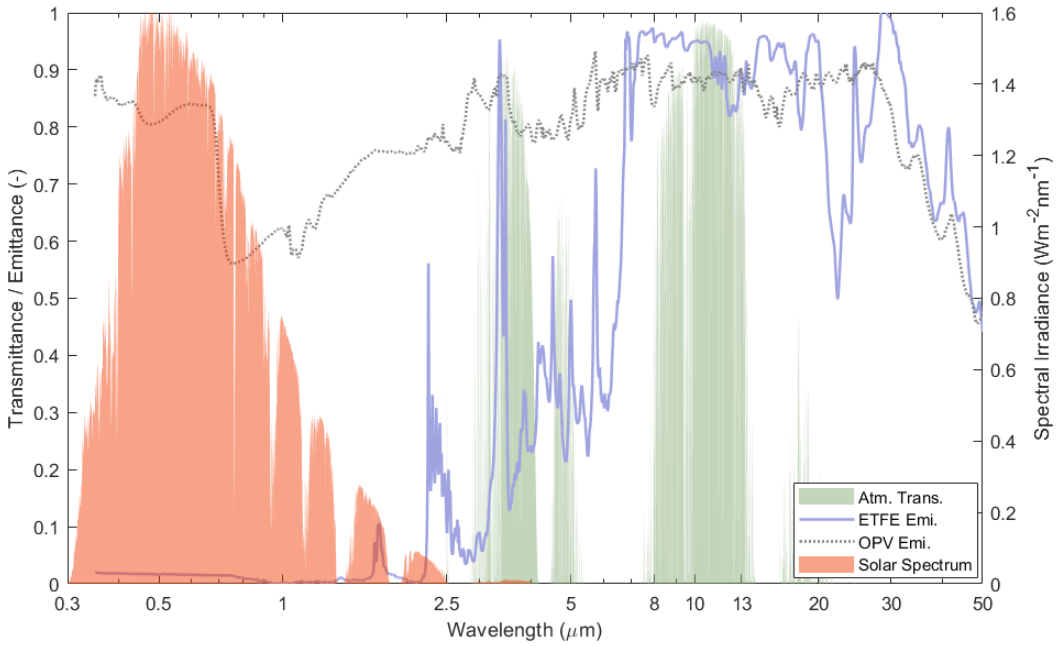

Figure 3. Spectral normal emittance of the ETFE foil (150 µm-thick) and the OPV module, spectral transmittance of the atmosphere, and AM1.5G solar radiation spectrum.

2.2 Modelling of the emittance of three-layer cushions

The spectral directional absorptance/emittance of the ETFE-OPV cushions was modelled over the same spectral range (0.35– 50 µm) using a 3D ray tracing algorithm programmed in Matlab. The code is formulated to consider all photonic interactions within the cushions.

The exact 3D geometry of commercially available ETFE cushions was modelled as depicted in Figure 4 [24]. The square cushions are 1 meter wide and have a height of 0.16 meters. The cushions are comprised of three layers where two of them act as shell elements (envelope, the top layer facing the outside of the building, and the bottom layer facing the inside) having the shape displayed in Figure 4 when inflated. The third middle layer splits the chamber into two.

Four different cushion configurations with different sets of ETFE and OPV layers were studied as described in Table 1:

Table 1. Set of studied cushion configurations.

Configuration	Layer		
	Top	**Middle**	**Bottom**
C0	ETFE	ETFE	ETFE
C1	OPVs	ETFE	ETFE
C2	ETFE	OPVs	ETFE
C3	ETFE	ETFE	OPVs

Configuration C0 stands for a cushion where the three layers are considered to be 150 µm-thick ETFE foils. This configuration is already commercially available and installed in several buildings worldwide, hence once again stressing the importance of the present work which considers properly its optical and thermal properties. Configuration C1 substitutes the EFTE outer layer by a continuous array of OPVs facing the sun directly. C2 configuration is with the middle layer made of OPVs, thus keeping the cushion envelopes with ETFE foils. Finally, configuration C3 substitutes the most inner layer (the one facing the building interior) with the OPVs array.

These configurations were selected in order to properly assess how incorporating OPVs in semi-transparent envelopes impacts its performances (optical, thermal and electrical output) and to determine the best position for the OPV module within the cushion. The electrical and thermal productions are closely related and depend on how the module is illuminated as a function of its position within the cushions.

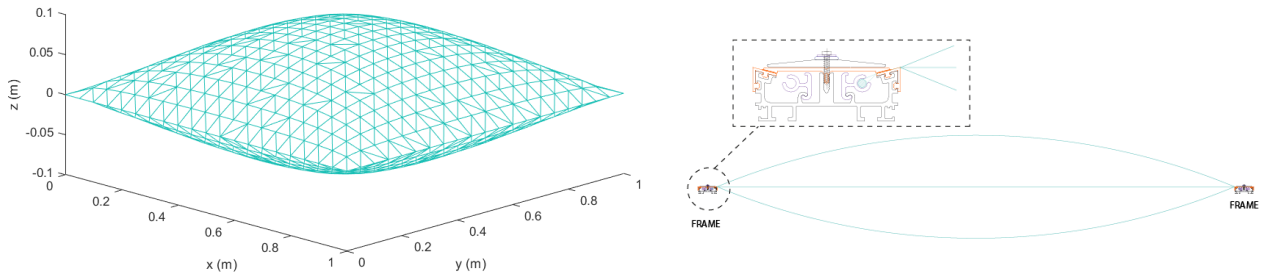

Figure 4. 3D exterior geometry of the cushion with the triangle meshing and cross-sectional view with a zoom on the fixing frame.

A meshing with triangles of the curved cushions was performed to compute the ray-tracing algorithm while considering the exact geometry. Consequently, surfaces were split into a set of small triangles that all together replicate the exact geometry.

The ray-tracing code is fed with the optical constants derived from the experimental measurements to determine the total emittance of the cushion and the emittance of each individual layer. It computes absorption within different layers as a function of randomly distributed points above the cushion where the rays are launched and randomly distributed incidence directions (zenith and azimuth). A uniform distribution of launching points above the cushion was considered to properly simulate radiative interactions between the different layers in the cushion. A sufficiently large number of rays was simulated using a Monte-Carlo approach to ensure that the results were converged.

2.3 Thermal model

A computational fluid dynamics (CFD) model was built in Comsol Multiphysics to simulate the thermal behaviour of the cushion. First, a two-layer ETFE cushion was modelled and experimentally validated. The simulation was conducted following the EN 673 regulation for glazing elements [25]. According to this regulation, the boundary conditions indicated in Figure 5 were assumed. The convective heat transfer coefficients were set at 7.7 W/(m^2K) and 25 W/(m^2K) for the internal and external ETFE layers, respectively. Indoor air temperature was set at 20 ºC and outdoor air temperature at 0 ºC. The ETFE emittance was calculated according to the EN 12898 regulation from spectral measurements and the directional values obtained from the emittance modelling described in the previous section. The resulting value, 0.839, was then introduced in Comsol [26]. Coupling of turbulent natural convection and thermal radiation is accounted for in the simulations. Later, the model was extended to a three-layer system with only ETFE layers (C0) and including the OPV module as top, middle or inner layer (Configurations C1-C3 in Table 1). The emittance of the OPV module was determined applying the same method as for the ETFE layer, resulting in a value of 0.846. It should be noted that both emittance values of the ETFE and the OPV module are quite similar since in the interval 7-50 μm their spectral emittances fall within the same range and the EN 12898 prioritizes this bandwidth in the calculation method.

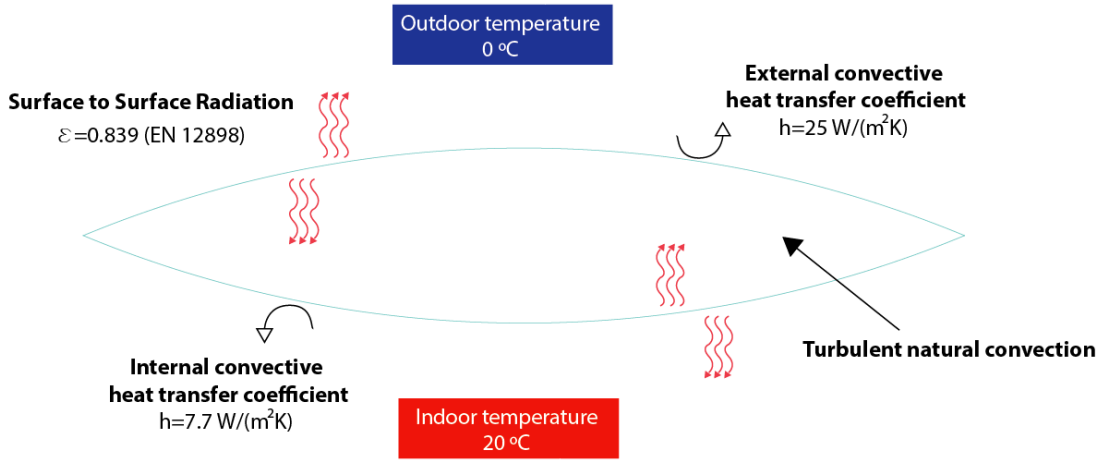

Figure 5. Boundary conditions for CFD simulations (Emittance value of the ETFE).

An experiment with a two-layer ETFE cushion placed horizontally was assembled in the laboratory, since this cushion configuration is the most usual installation in real buildings [24]. The experimental setup had only 2 layers of ETFE instead of 3, because it was not possible to maintain the pressure adequately with 3 layers. Heat flux (Hukseflux®) and several temperature (T-type thermocouples) sensors were installed to measure the flux passing through the walls (Qw) and the ETFE layers, and interior (Ti) and exterior (Te) temperatures. The 1x1x1 m^3 cubicle where the ETFE was installed at the top had 0.15 m-thick insulated walls. Figure 6 shows a schematic and a picture of the experimental setup. In the picture, the blowing unit to keep the air pressure inside the cushion and the data acquisition system (DAQ) system are visible. From the experiment, the thermal transmittance (U) was obtained by calculating the heat flux passing through the cushion as the difference between the heat flux of the electric resistor (Qh) and the heat flux passing through the walls (Qw):

$$U = \frac{Qh - Qw}{(Ti - Te)A} \quad (2)$$

where A is the aperture area of the cushion.

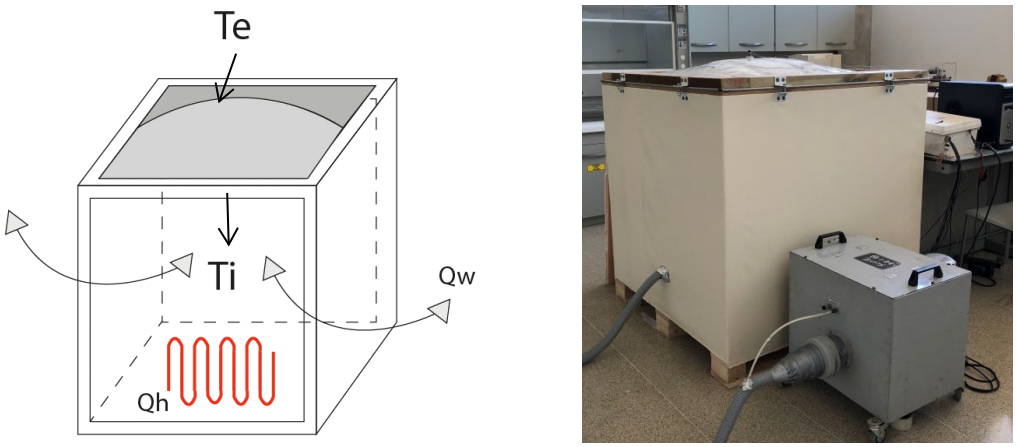

Figure 6. Schematic and photograph of the experimental setup.

3 Results

This section describes the main optical, thermal and electrical performances of the OPV-ETFE cushions.

3.1 Optical performance

In this subsection, the optical performance of the four selected configurations is assessed. It should be noted that, as previously remarked, the absorptance and the emittance are named indistinctly.

The first results shown in Fig. 7 are about the reference configuration consisting of three ETFE layers. Since all the layers are ETFE foils, the cushion in this configuration is highly transmissive over the solar range with an average value of 0.8. On the other hand, the cushion is highly absorptive in the mid-infrared above 7 μm, and in particular over the atmospheric transparency window (8-13 μm). These two behaviors are key, in the infrared for radiative cooling purposes and for ensuring high transparency over the solar range for lighting purposes.

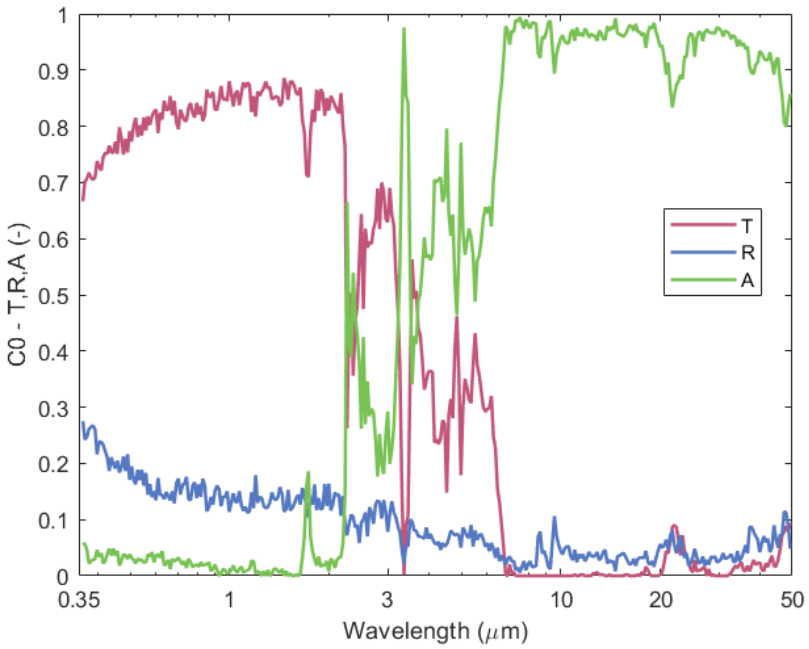

Figure 7. Spectral reflectance, transmittance and absorptance of the three-layer cushion in configuration C0 (under normal incidence).

Figure 8 displays the reflectance transmittance, and absorptance for configurations C1, C2 and C3. Several differences with Figure 7 can be identified. Cushions including OPVs (regardless of its position) become much more absorptive in the solar range. The three configurations (C1, C2 and C3) show similar overall reflectance, absorptance and transmittance with minor differences. These cushions are transmissive from 0.7 to 1 μm with peaks of transmittance not higher than 0.35.

On the other hand, there are some differences between C1, C2 and C3 when looking at the absorptance of the OPVs. As expected, in the configuration where the module is placed at the outer layer (C1), OPVs absorb more solar irradiation and thermal radiation. In configuration C2, OPVs still absorb most of the solar irradiation due to the high ETFE transmittance (0.08 less than in configuration C1) while most of the thermal mid-infrared radiation coming from the atmosphere is absorbed by the outer layer. Finally, configuration C3 follows the same trend but, since solar irradiation has to cross two ETFE layers before impacting the module, the amount of solar radiation absorbed is reduced by approximately 0.2 compared to configurations C1 and C2. In addition, the amount of infrared thermal radiation reaching the module is very low.

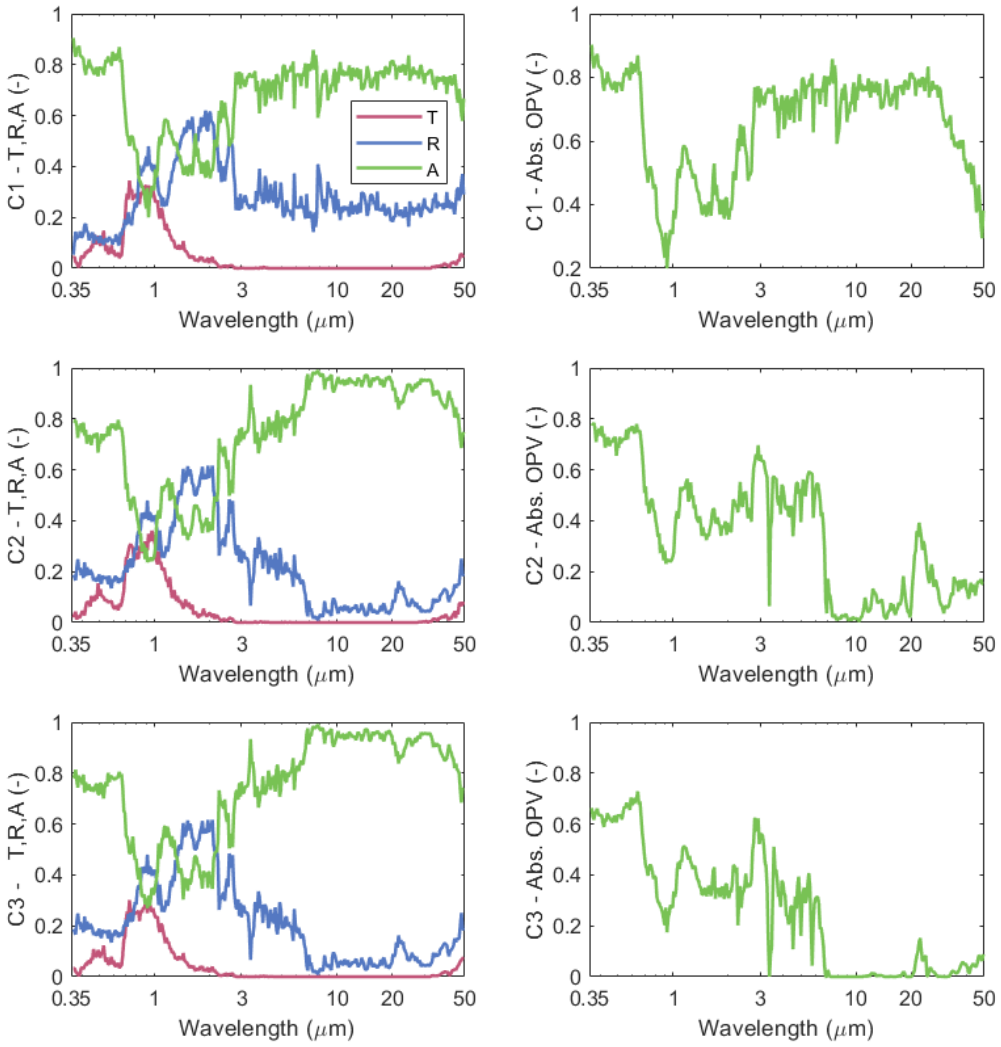

Figure 8. Spectral reflectance, transmittance and absorptance of the three-layer cushion in configurations C1, C2 and C3 together with the OPVs' absorptance in each configuration (under normal incidence).

Although in the present study spectral transmittance, reflectance and absorptance values are shown under normal incidence of the solar radiation, by utilizing the emittance model based on ray tracing, these values could also be provided for any arbitrary sun rays' angle of incidence (or location, position and orientation of the cushion) in order to analyze a particular building installation in a given city, for instance.

3.2 Thermal performance

Figure 9 displays the temperature contours and the velocity streamlines of air enclosed between the foils. The cavity, with the hotter temperature at the bottom, experiences natural Rayleigh-Bénard convection. In the velocity streamlines graph, the Bénard cells can be clearly identified.

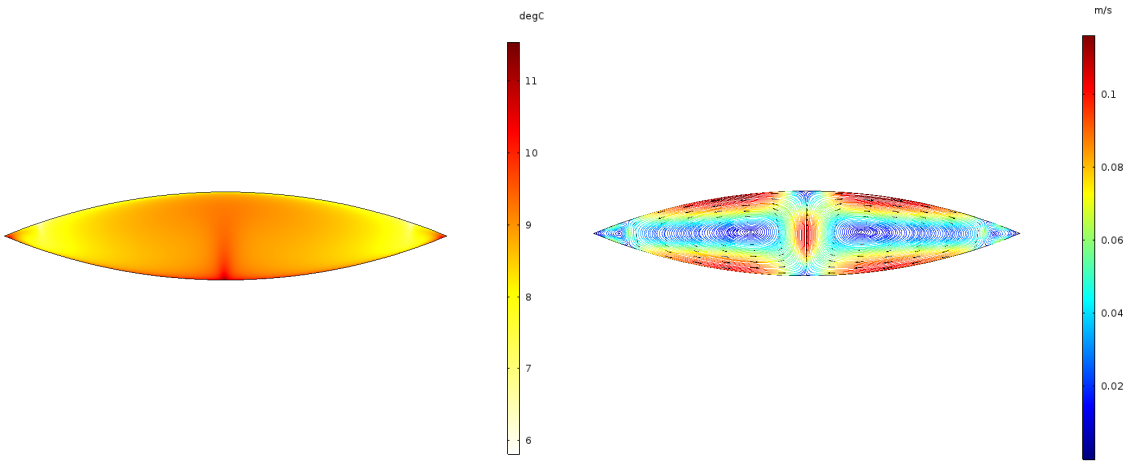

Figure 9. 2-layer cushion air temperature contours and velocity streamlines.

With these results, the mean thermal transmittance coefficient for a 2-layer cushion placed horizontally was found to be $U = 2.65$ W/ m^{2}K. This result was experimentally validated with the experimental setup described in the previous section. Figure 10 (left) illustrates the monitored temperatures of the interior (bottom) and exterior (top) ETFE layers. When the electrical resistor is on, the interior temperature experiences a linear increase. However, the exterior temperature follows a periodical trend. It increases up to certain point when suddenly it decreases before starting the same cycle again. This behavior was due to the pump blowing air to keep the pressure constant. When the pressure sensor detected a decrease in pressure, fresh air from outside was blown in, thus provoking the observed effect. The heat flux was calculated for several cycles, getting the tendency included in Fig. 10 (right).

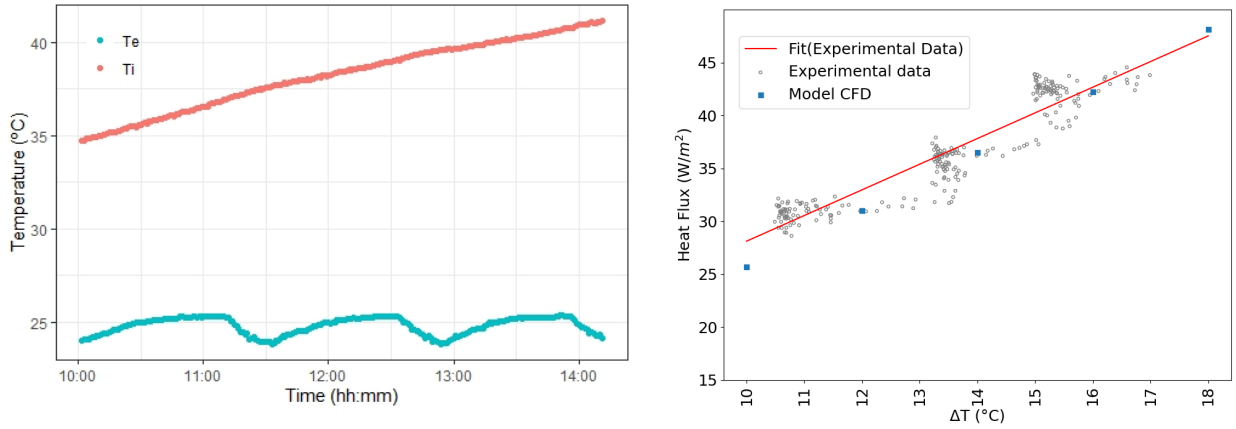

Figure 10. Left: Interior and exterior temperatures in the test unit; Right: heat flux crossing the cushion as a function of the interior and exterior temperatures difference.

The slope of the heat flux vs. temperature difference curve is the mean thermal transmittance, which is 2.70 W/ m^{2}K. The relative difference between this value and the result from the CFD simulations (2.65 W/ m^{2}K) is less than 2%, meaning a very good agreement.

Considering that the CFD model is validated, the following results deal with the temperature distributions for the 3-layer configurations C0-3. The boundary conditions are the same as for the 2-layer case, as indicated by the norm [25].

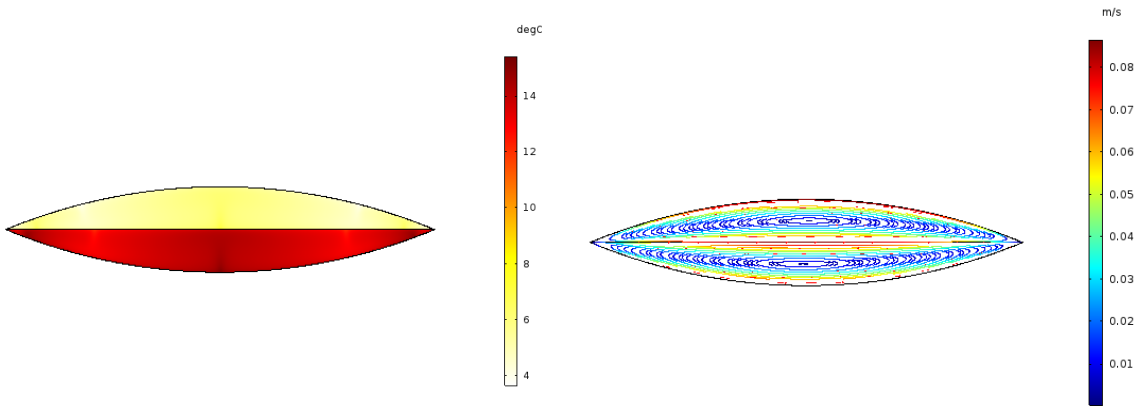

Figure 11. 3-layer cushion (C0) air temperature contours and velocity streamlines .

Temperature contours and velocity streamlines considerably change with respect to the previous configuration since the middle layer creates two different temperature zones and splits the two Bénard cells into one per cavity. In this configuration, the thermal transmittance is decreased to 1.58 W/ m^{2}K. This value is similar to that of very high quality double glass windows with air cavities between 6 mm glass panes of about 16 mm. However, in the case of

the ETFE cushions, the foil thickness is 150 μm compared to the 6 mm of glass and, in addition, the density of ETFE is half of that of glass. Moreover, using ETFE allows manufacturing glazing elements up to about 6 m by 3 m per framing structure. Since the energy required for fabrication and recycling is much less than that for glass, the associated environmental costs are lower [14].

The mean temperatures of the layers are 4.5 ºC for the external layer, 9.3 ºC for the middle layer and 14.1 ºC for the internal layer. It should be noticed that, following the European regulation [25], simulations neither consider the solar spectrum nor thermal radiation effects (internal heat sources within the foils due to radiation exchange). Therefore, since the calculations deal with temperatures only in the range [0-20] ºC and the emittance values of OPV module (0.846) and ETFE (0.839) are quite similar, the thermal transmittances obtained are almost the same for the three-layer cushion configurations, with a maximum difference of only 0.5% between the lowest and the highest thermal transmittance values.

3.3 Electrical performance

Figure 12 (left) shows the solar irradiance absorbed by the OPVs in the spectral range where photogeneration takes place. Ideally, high irradiance is desirable over this range and radiation absorbed outside this range will just heat up the module.

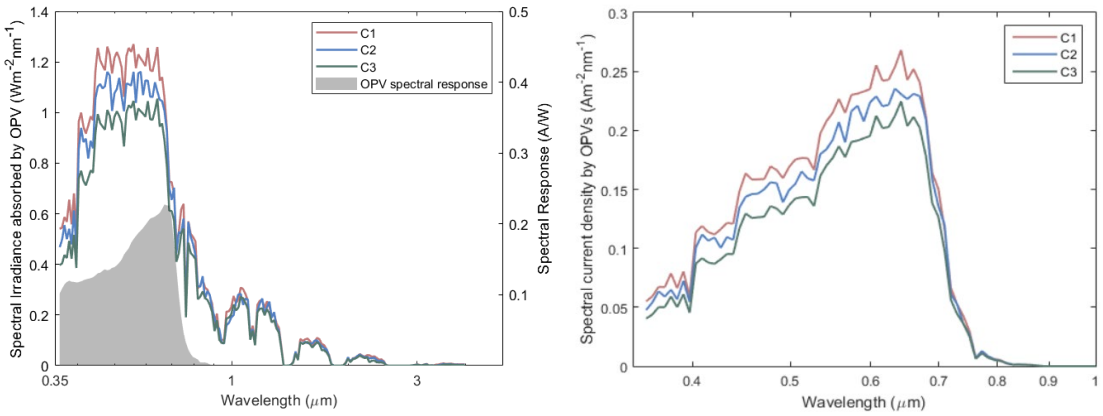

Figure 12. Left: Solar Irradiance absorbed by OPVs in configurations C1, C2 and C3; Right: Spectral short-circuit current density (J_{sc}) in configurations C1, C2 and C3 (under normal incidence).

By integrating the spectral short-circuit current (calculated by multiplying the OPV spectral response with the spectral radiation absorbed by the OPV) from Fig. 12 (right), the short-circuit

current density can be obtained. Results, given in Table 3, are consistent with the region of OPVs' absorptance spectra (Figure 8) where the photovoltaic effect takes place. However, OPVs' absorptance in the mid-infrared is also increasing as the OPVs are moved from the top (configuration C1) to the bottom (C3), meaning absorption of radiation that heats up the layers.

Table 3. Short-circuit current density (J_{sc}) in configurations C1, C2 and C3.

	J_{sc} (Am^{-2})
C1	65.17
C2	59.85
C3	53.39

Selection of the best cushion configuration should consider the dependence of electrical production of the OPV module on temperature of the layer where it is placed. For temperatures ranging from 15 to 35 ºC, the higher the temperature the higher the power of OPV modules. From 35 ºC to 45 ºC and for incident irradiance values higher than 200 W/m^2, the maximum power tends to decrease or to stabilize but never achieves values lower than those obtained at 15 ºC [27]. Based on that fact, the best configuration for PV production is that delivering the maximum current density independently of temperature of the module (C1) in the operating temperature range [15-45] ºC. This assumption is supported by the experimental study conducted in [28], where maximum temperatures of 55 ºC were found for several OPV modules tested at ambient temperatures achieving a maximum close to 40 ºC, which is considered as a high temperature value. Therefore, the obtained results leading to position the OPV modules in the configuration achieving the highest irradiance values is considered valid for a wide range of operating conditions. On the other hand, it should be noted that for temperatures above 45 ºC, the module degradation could increase considerably [27]. Regarding light-induced module degradation, mainly caused by the UV radiation fraction, the effect would not be different as a function of the OPV layer position in the three-layer cushion since ETFE is transparent to UV. In any case, a UV-filter layer is recommended for OPV modules to avoid degradation, especially in those with fullerene-base acceptors [29].

4 Conclusions

Spectral transmittance and reflectance values of ETFE foils with different thicknesses and of a commercially available OPV module have been measured from 0.35 μm to 50 μm, covering

from the far ultraviolet, visible and mid-infrared regions. This radiative characterization allows covering more than 99% of the spectrum emitted by a blackbody at a temperature of 25 ºC.

Spectral emittances, calculated by ray-tracing from using the optical properties (complex refractive index) inferred from measured optical characteristics, are reported for four different horizontal three-layer cushion configurations. Configuration C0 refers to a three-layer ETFE cushion and C1-C3 are with three layers but with two layers of ETFE and one consisting of an OPV module. Position of the OPV layer is either at the top (C1), or at the bottom (C3), or in the middle (C2). C0 is highly emissive in the mid-infrared, with an almost 100% emittance over the atmospheric transparency window (8-13 μm), and transmits almost entirely the solar spectrum. Cushions including OPVs (regardless of its position) become much more absorptive in the solar range. The three configurations (C1, C2 and C3) show similar overall reflectance, absorptance and transmittance with minor differences. Regarding the OPV layer, the configuration where the module is at the top (C1) is that with the largest irradiation absorbed by OPVs, including the solar fraction.

The CFD model results in thermal transmittances of 2.65 W/m^2K and 1.58 W/m^2K for the two- and three-layer cushions. In the case of the two-layer ETFE cushion, numerical results were experimentally validated showing a very good agreement. Regarding the three-layer configuration, the mean temperatures of the three layers obtained through the numerical simulations are 4.47 ºC, 9.27 ºC and 14.07 ºC, referred from top (outer) to the bottom (inner) layers, assuming that outdoor and indoor temperatures are 0 °C and 20 °C, respectively.

Electrical performance of the OPV module is influenced by the position of the module. Short-circuit current densities range from around 50 A/m^2 to 65 A/m^2 for the worst and best case.

The thermal results obtained reveal a great potential of this type of glazing for building integration applications since thermal transmittances are similar to those of very high quality double-glass windows. However, in terms of weight, manufacturability and economical and environmental costs, ETFE may be advantageous.

Further investigations have to be carried out to fabricate a real-size ETFE/OPV cushion to be characterized outdoors in a test unit. They will complement the results obtained in the laboratory. CFD modelling could be improved by including the solar spectral irradiance and radiative exchanges with the cold outer space in clear-sky conditions.

Acknowledgements

This research was supported by the "Generalitat de Catalunya" (2017 SGR 1276 and ICREA Academia) and "Ministerio de Ciencia e Innovación" of Spain (grant reference PID2019-111536RB-I00). The authors would like to acknowledge the collaboration with the company IASO SA.

5 References

[1] European Parliament, "The energy performance of buildings directive factsheet (2019)." .

[2] H. Khandelwal, A. P. H. J. Schenning, and M. G. Debije, "Infrared Regulating Smart Window Based on Organic Materials," *Adv. Energy Mater.*, vol. 7, no. 14, 2017.

[3] A. Cannavale, F. Martellotta, F. Fiorito, and U. Ayr, "The challenge for building integration of highly transparent photovoltaics and photoelectrochromic devices," *Energies*, vol. 13, no. 8, 2020.

[4] DIRECTIVE (EU) 2018/844, "Directive 2018/844/EU Energy performance of buildings," *Off. J. Eur. Union*, vol. 2018, no. October 2012, pp. 75–91, 2018.

[5] P. K. Nayak, S. Mahesh, H. J. Snaith, and D. Cahen, "Photovoltaic solar cell technologies: analysing the state of the art," *Nat. Rev. Mater.*, vol. 4, no. 4, pp. 269–285, 2019.

[6] K. Lee *et al.*, "The Development of Transparent Photovoltaics," *Cell Reports Phys. Sci.*, vol. 1, no. 8, p. 100143, 2020.

[7] G. P. Kini, S. J. Jeon, and D. K. Moon, "Latest Progress on Photoabsorbent Materials for Multifunctional Semitransparent Organic Solar Cells," *Adv. Funct. Mater.*, vol. 31, no. 15, pp. 1–32, 2021.

[8] S. Lizin *et al.*, "Life cycle analyses of organic photovoltaics: A review," *Energy Environ. Sci.*, vol. 6, no. 11, pp. 3136–3149, 2013.

[9] S. Robinson-Gayle, M. Kolokotroni, A. Cripps, and S. Tanno, "ETFE foil cushions in roofs and atria," *Constr. Build. Mater.*, vol. 15, no. 7, pp. 323–327, 2001.

[10] S. Afrin, J. Chilton, and B. Lau, "Evaluation and comparison of thermal environment of atria enclosed with ETFE foil cushion envelope," in *Energy Procedia*, 2015, vol. 78, pp. 477–482.

[11] M. Schäffer and B. Stimpfle, "Large scale ETFE cushion roof covers the Lilienthalhaus in Brunswick, Germany | ETFE-Großkissendach über dem Lilienthalhaus in Braunschweig," *Stahlbau*, vol. 87, no. 7, pp. 649–656, 2018.

[12] L. S. Babayan, *ETFE plastic application for reconstruction and preservation of architectural structures in Syunik Province, RA*, vol. 828 KEM. 2020.

[13] M. Rychtáriková, R. Šimek, J. Húsenicová, and V. Chmelík, "Prediction of noise levels in large shopping streets covered by glass and ETFE," *Archit. Eng. Des. Manag.*, 2020.

[14] C. Lamnatou, A. Moreno, D. Chemisana, F. Reitsma, and F. Clariá, "Ethylene

tetrafluoroethylene (ETFE) material: Critical issues and applications with emphasis on buildings," *Renew. Sustain. Energy Rev.*, vol. 82, pp. 2186–2201, 2018.

[15] A. Zanelli, P. Beccarelli, C. Monticelli, and H. M. Ibrahim, "Technical and Manufacturing Aspects in order to create a smart façade system with OPV integrated into ETFE foils," vol. 2, no. May, 2012.

[16] Z. Fan, M. De Bastiani, M. Garbugli, C. Monticelli, A. Zanelli, and M. Caironi, "Experimental investigation of the mechanical robustness of a commercial module and membrane-printed functional layers for flexible organic solar cells," *Compos. Part B Eng.*, vol. 147, no. August 2016, pp. 69–75, 2018.

[17] J. Hu *et al.*, "Electrical-thermal-mechanical properties of multifunctional OPV-ETFE foils for large-span transparent membrane buildings," *Polym. Test.*, vol. 66, pp. 394–402, 2018.

[18] A. Menéndez *et al.*, "A multifunctional ETFE module for sustainable façade lighting: Design, manufacturing and monitoring," *Energy Build.*, vol. 161, pp. 10–21, 2018.

[19] Á. Moreno, D. Chemisana, R. Vaillon, A. Riverola, and A. Solans, "Energy and luminous performance investigation of an OPV/ETFE glazing element for building integration," *Energies*, vol. 12, no. 10, 2019.

[20] InfinityPV, "InfinityPV foil," *OPV brochure*, 2020. [Online]. Available: https://infinitypv.com/. [Accessed: 20-May-2020].

[21] D. Zhao *et al.*, "Radiative sky cooling: Fundamental principles, materials, and applications," *Appl. Phys. Rev.*, vol. 6, no. 2, 2019.

[22] T. P. Otanicar, P. E. Phelan, and J. S. Golden, "Optical properties of liquids for direct absorption solar thermal energy systems," *Sol. Energy*, vol. 83, no. 7, pp. 969–977, 2009.

[23] ASTM, "G173-03 Standard tables for reference solar spectral irradiances: direct normal and hemispherical on 37° tilted surface," *B. Stand.*, vol. 14.04, 2004.

[24] Iasoglobal, "Iasoglobal ETFE cushion," *ETFE cushion brochure*. [Online]. Available: https://www.iasoglobal.com. [Accessed: 15-Nov-2019].

[25] AENOR, "UNE EN 673:2011. Vidrio en la construcción. Determinación del coeficiente de transmisión térmica U. Método de cálculo.," 2011.

[26] EN, "12898. GLASS IN BUILDING. DETERMINATION OF THE EMISSIVITY.," 2001.

[27] G. Bardizza, E. Salis, and E. D. Dunlop, "Power matrix of OPV mini-module under steady conditions of temperature and irradiance at large-area solar simulator," *Sol. Energy*, vol. 204, pp. 542–551, 2020.

[28] D. Chemisana *et al.*, "Performance and stability of semitransparent OPVs for building integration: A benchmarking analysis," *Renew. Energy*, pp. 177–188, 2019.

[29] J. B. Patel *et al.*, "Effect of Ultraviolet Radiation on Organic Photovoltaic Materials and Devices," *ACS Appl. Mater. Interfaces*, vol. 11, no. 24, pp. 21543–21551, 2019.